

Dual Side Polished PCF Based Surface Plasmonic Refractive Index Sensor for Detection of Water Pollution

Md. Kamrujjaman*, Md. Anwar Hossain*, Nguyen Hoang Hai[†], and Feroz Ahmed[§]

* Department of Electrical and Electronic Engineering, Bangladesh University of Business and Technology, Bangladesh

[†]School of Electronics and Telecommunication, Hanoi University of Science and Technology, Vietnam

[§] Department of Electrical and Electronic Engineering, Independent University of Bangladesh, Bangladesh
Email: ksujon760@gmail.com, anwar.ee113@ieee.org, hai.nguyenhoang@hust.edu.vn, fahmed@iub.edu.bd

Abstract— In this work, a photonic crystal fiber (PCF) based surface plasmon resonance (SPR) sensor has been designed for water pollution detection. Using the finite element method (FEM), the performance of a dual-side polished PCF has been investigated and reported. The plasmonic material for this design is a thin silver (Ag) layer deposited outside the PCF framework. In addition, a thin layer of Titanium Oxide (TiO₂) was added to protect the silver layer from oxidation. Utilizing the wavelength interrogation method in the sensing range of RI 1.31-1.35, the proposed sensor shows a maximum sensitivity of 3000 nm/RIU at a silver layer thickness of 40 nm. A sensitivity of 2250 nm/RIU was obtained, particularly in the specific value of RI-1.33. Furthermore, a maximum sensitivity of 475 RIU⁻¹ and a maximum sensor resolution of 5.83×10⁻⁶ RIU were obtained utilizing the amplitude interrogation method. Since the sensor has a sensing range of 1.31 to 1.35 with high sensitivity, it would be a great option for biosensing, organic chemical sensing, and other analytes detection in that range.

Keywords—component, formatting, style, styling, insert (key words)

I. INTRODUCTION

Surface plasmon resonance is one of the most intriguing and exciting technology in the field of sensor. Most innovative optoelectronic sensors generally use this sensing technology to detect different analyte. But most of them use prisms or other moving mechanical arrangements to generate SPR. And these arrangements make the system costly and bulky [1]. In recent years a lot of researchers have taken a great interest on PCF-based SPR sensor due to its high sensitivity, high resolution and real time detection facility. PCF based SPR sensors are currently widely employed in a variety of sensing applications, including environmental monitoring, food standards, hydrostatic testing, fluid detection, gas detectors, biomedical applications, and clinical applications, such as pharmaceutical detection, biomedical imaging, physiological analyte, and biochemical detection [1].

PCF based SPR use the surface plasmon waves (SPW), which results from the collective oscillation of plasmons (e⁻) in the metal-dielectric interface [3]. These SPWs can be formed into travelling wave and direct them to the metal-dielectric layer known as surface plasmon polariton (SPP) [4]. SPPs are developed by coupling the electromagnetic field and plasmons (electrons) of plasmonic materials like Ag, Au, Al, Cu, etc. [1]. When frequency of incident light equals the frequency of SPWs, resonance occurs as these two waves reach phase-matching condition. In this condition, a strong bonding is established between the fundamental core mode and the plasmonic mode (SPP mode), resulting maximum transfer of light energy from the core mode to the SPP mode.

During this phenomenon, a peak loss appears for a particular analyte or refractive index. Any changes to the analyte refractive index results in peak loss wavelength shifting [1,3,4]. PCF based SPR sensor detect the shifting of the resonance wavelength hence, senses the RI change [4].

Suitable material selection for plasmonic layer is a major point in PCF based SPR sensing. A number of plasmonic materials are used in earlier research works like Au [3,18], Ag [1], Al, TCOs [6] etc. Among these materials, transparent conducting oxides (TCOs) exhibit good results in near-infrared range. In recent times Au is used mostly because of its good plasmonic behavior and does not have oxidation problem. But in the visible range, Ag shows excellent plasmonic behavior along with extreme sensitivity and sharp resonance peak [18]. But it has oxidation problem, although it can be overcome by adding extra layer of titanium oxide or graphene. furthermore, different types of PCF-SPR sensor designs have been proposed in recent papers such as microchannel based [1], H-shaped [19], hollow core [4], solid core [18], D-shaped [2], dual core [3] etc. These designs are not rigid model and can be modified. The shape of the lattice configuration varies from papers to papers to fulfil the requirements of that particular paper. These sensors can be classified into two types (internally deposited and externally deposited) considering the deposition of plasmonic material [4].

In this work, a dual side polished circular lattice PCF based surface plasmonic RI sensor is proposed to enhance the sensitivity particularly at RI-1.33 (RI of Water) and adjacent range. Since most of the organic chemicals, biological analytes and pharmaceutical materials etc. are lies between this sensor's sensing range, this sensor will be a great option for sensing those analytes. This sensor is analyzed by finite element method (FEM) based COMSOL Multiphysics software. Both x-polarized and y-polarized core modes are analyzed. The external deposition of plasmonic material Ag and TiO₂ reduces fabrication difficulties and enhance sensing performance. Furthermore, Ag layer and TiO₂ layer thickness along with airhole pitch and diameter tuned to extract the best possible result.

The 4th Industrial Revolution or industry 4.0 is highly dependent on sensors (like PCF-SPR-based sensors). Condition-monitoring is one of the important element in modern industry and sensors plays a vital role in there as they are used to monitor the entire manufacturing process. This work is also related to industry 4.0 because the proposed sensor can be used as a condition-monitoring tool for various industries. Any industry using water or analyte ranging between RI 1.31 to 1.35 in the manufacturing process can use

this proposed sensor for continuous monitoring, data collection, and further decision-making.

II. NUMERICAL DESIGN AND MODELING

Fig. 1 represented the proposed sensor's schematic design. The air holes are arranged in two circular arrays. The center most air hole is there to form a dual core light confinement phenomenon. The pitch is "A" in every direction, where $A=2\mu\text{m}$. There are four types of air hole diameter is used, they are $d_c=0.6\mu\text{m}$, $d_s=0.25\mu\text{m}$, $d_1=1\mu\text{m}$, $d_2=1.2\mu\text{m}$. PCF's two side is polished and coated with Ag and TiO_2 to form a detection layer. The air holes are assembled in such a way that light will propagate in the polished side to maximize the desired output. The first circular airhole array is positioned from the center airhole at "A" distance. This array's two airhole positioned at 0° and 180° degree is removed to concentrate the maximum amount of light in that region. The second circular airhole array is positioned at "2*A" distance from center airhole. Again, the second array's two airhole positioned at 0° and 180° degree is scaled down to guide the light in the sensing layer. A circular channel is created outside the arrangement to host the analyte with diameter of $2.3\mu\text{m}$. The diameter of the PML layer is set to $1.2\mu\text{m}$.

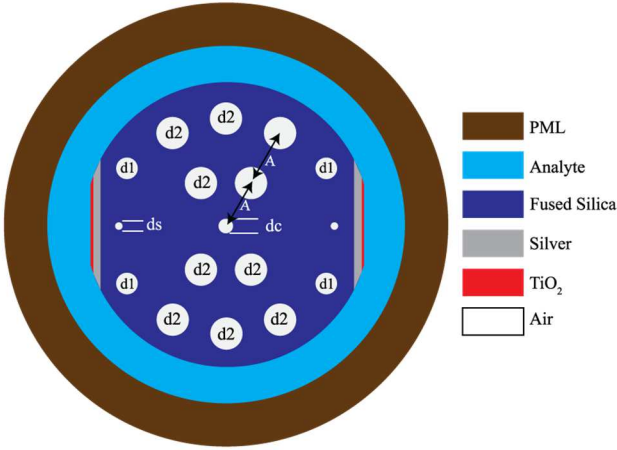


Fig. 1. Schematic diagram of proposed sensor

Fused silica serves as the sensor's ground material. The following Sellmeier equation is used to calculate the refractive index of fused silica as mentioned in [1,3],

$$n_{s_i}^2(\lambda) = 1 + \frac{B_1\lambda^2}{\lambda^2 - C_1} + \frac{B_2\lambda^2}{\lambda^2 - C_2} + \frac{B_3\lambda^2}{\lambda^2 - C_3} \quad (1)$$

Where, n is the λ -dependent refractive index of fused silica, and λ is the wavelength in μm . B_1 , B_2 , B_3 , C_1 , C_2 , and C_3 are the Sellmeier constants[3].

To reduce adhesion and improve sensitivity, a thin coating of Titanium Oxide (TiO_2) is placed over the silver layer. The Titanium Oxide layer also aided in the efficient stimulation of the SPR and the interface of the core-guided mode to the SPP mode. The following equation is used to calculate the dielectric constant of titanium oxide [5],

$$n_{\text{TiO}_2}^2 = 5.913 + \frac{2.441 \times 10^7}{(\lambda^2 - 0.803 \times 10^7)} \quad (2)$$

Where, n is the refractive index of Titanium oxide which changes with respect to wavelength.

III. RESULT AND PERFORMANCE ANALYSIS

Fig. 2a – 2c exhibit the mode field patterns of the fundamental x-pol and y-pol modes, as well as the y-pol of the SPP mode. Due to missing air gaps in the first circular array, the proposed PCF exhibits birefringence, inducing N_{eff} among the x-polarization and y-polarization core modes.

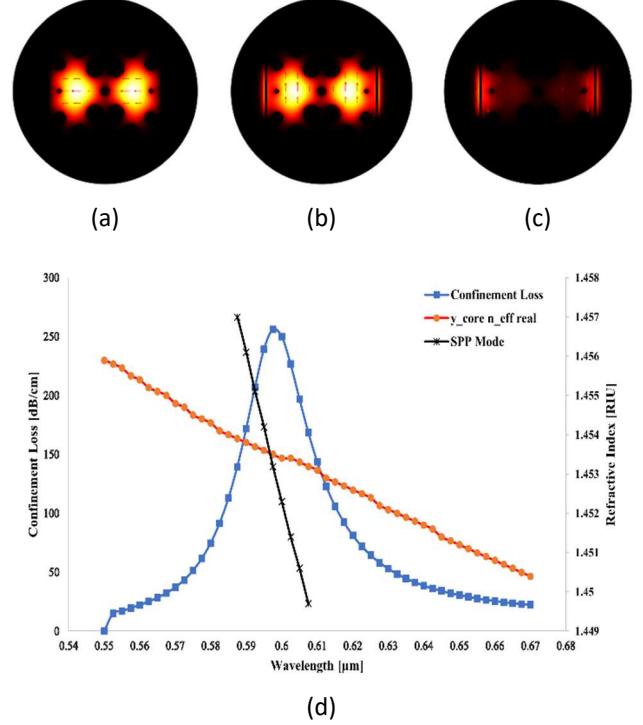


Fig. 2. At $0.5975\mu\text{m}$, (a) x-pol core mode, (b) y-pol core mode, and (c) y-pol SPP mode. (d) The dispersion relationship uniting the fundamental core-guided mode and the SPP mode with $n_a = 1.33$ and $t_s = 40\text{nm}$.

Fig. 2d shows the phase matching for analyte having RI 1.33. The real part of y-pol core and SPP-mode coincide with one another at $0.5975\mu\text{m}$, as seen in the figure. This is the resonance condition (phase matching point) and the resonance wavelength is $0.5975\mu\text{m}$. A sharp peak can be seen at this wavelength, which reflects the maximum energy transfer from core guided mode to SPP mode.

Fig. 2b, y-pol core mode exhibits strong e-field near the metal-dielectric interface; as a result, the evanescent field interacts easily with the outer sensing layer. [3,13]. Therefore, chances of coupling with surface electrons are low for this mode. The surface electrons of silver are hence strongly connected to the y-pol core mode [13]. So, y-pol core mode is more effective for this sensor's performance study [1,3].

The Confinement Loss is an important factor to consider when evaluating sensor performance [1]. The following equation can be used to calculate confinement loss [1,3,10-12],

$$\alpha(\text{dB/cm}) = 8.686 \times k_o \text{Im}(n_{eff}) \times 10^4 \quad (3)$$

Where, $k_o = 2\pi/\lambda$ is the number of wave in the free space, $\text{Im}(n_{eff})$ is imaginary part of the effective RI and λ is the operating wavelength.

For RI 1.33 maximum loss of 256.03dB/cm is obtained at resonance point for $0.5975\mu\text{m}$. The real part of the SPP mode's n_{eff} is significantly reliant on analyte's RI fluctuation.

A little change in analyte's RI causes a change in n_{eff} , which causes the phase matching point to shift towards other resonance wavelengths. Fig. 3 depicts the shifting phase matching points caused by a change in analyte level from 1.31 to 1.36.

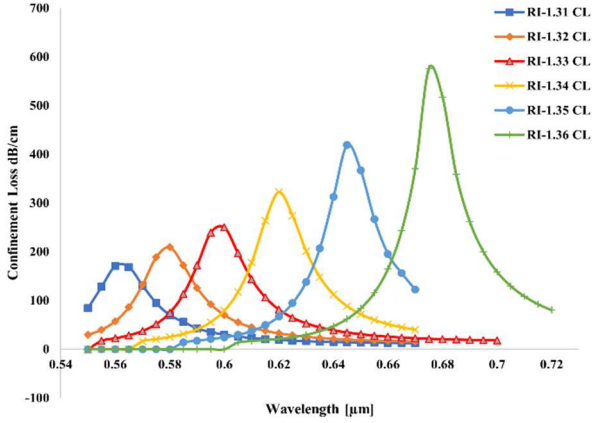


Fig. 3. Variation in confinement loss for increasing analyte RI from 1.31 to 1.36

From Fig. 3, it is obvious that increasing the analyte RI value induces red shifting, or a shift in resonance wavelength to a greater wavelength. Due to the change of analyte's RI from 1.31 to 1.32, 1.32-1.33, 1.33-1.34, 1.34-1.35, and 1.35-1.36, resonance wavelengths (λ) are shifted to 0.56–0.58 μm , 0.58–0.5975 μm , 0.5975–0.62 μm , 0.62–0.645 μm , and 0.645–0.675 μm , respectively. Fig. 3, also shows the magnitude of CL increases with the increase of analyte RI because when the analyte's RI is increased, core region and cladding region index contrast is reduced, hence resulting increase in CL.

The following equation can be used to calculate amplitude sensitivity [3]:

$$S_A(RIU^{-1}) = -\frac{1}{\alpha(\lambda, n_a)} \frac{\partial \alpha(\lambda, n_a)}{\partial n_a} \quad (4)$$

Where, overall propagation loss at RI of n_a is $\alpha(\lambda, n_a)$, change in analyte is δn_a and $\partial \alpha(\lambda, n_a)$ is the loss difference between two loss spectra.

For various RI analytes, the designed sensor's amplitude sensitivity is demonstrated below,

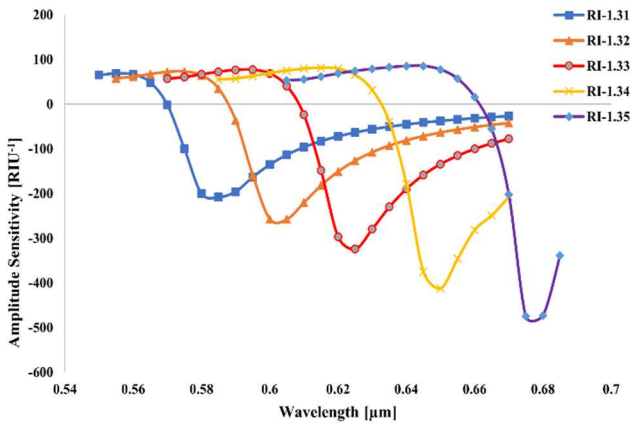


Fig. 4. Amplitude sensitivity for various analyte RI with $A=2\mu\text{m}$, $d_c=0.6\mu\text{m}$, $d_s=0.25\mu\text{m}$, $d_1=1\mu\text{m}$, $d_2=1.2\mu\text{m}$ & $t_s=40\text{ nm}$.

For analyte having RI of 1.35, we found a maximum S_A of 475 RIU^{-1} at 0.675 μm and a minimum S_A of 208 RIU^{-1} at 0.585 μm . At 0.625 μm , RI-1.33 had a maximum S_A of 324 RIU^{-1} .

The wavelength sensitivity can be calculated using the following formula [3,13]:

$$S_\lambda(\text{nm}/RIU) = \Delta \lambda_{peak} / \Delta n_a \quad (5)$$

The proposed sensor exhibits a $\Delta \lambda_{peak}$ of 20 nm, 17.5 nm, 22.5 nm, 25 nm and 30 nm for Δn_a of 0.01, where changes in RI are 1.31-1.32, 1.32-1.33, 1.33-1.34, 1.34-1.35, and 1.35–1.36. As a result, the calculated S_λ are 2000, 1750, 2250, 2500 and 3000 nm/RIU, respectively. The maximum wavelength sensitivity for RI-1.33 is 2250 nm/RIU.

Another essential variable is the sensor's resolution, which indicates how sensitive the sensor is to minor changes in analyte RI. The proposed sensor's resolution can be determined using the formula below [3,5]:

$$R(RIU) = \Delta n_a \times \Delta \lambda_{min} / \Delta \lambda_{peak} \quad (6)$$

Assuming, $\Delta n_a = 0.01$, $\Delta \lambda_{min} = 0.0175$, and $\Delta \lambda_{peak} = 30\text{ nm}$, we found the resolution to be as 5.83×10^{-6} RIU, which is comparable with [1,4,20,21]. As a result, even minor changes in RI levels on the order of 10^{-6} can be detected with excellent precision.

TABLE I. PERFORMANCE COMPARISON OF THE PROPOSED SENSOR WITH PREVIOUS PAPERS

Ref.	$S_A(RIU^{-1})$	$S_w(\text{nm}/RIU)$	Resolution	RI Range
[1]	2452	116,000	5.55×10^{-6}	1.29-1.39
[4]	266	2200	3.75×10^{-5}	1.33-1.36
[6]	1872	51000	9.09×10^{-6}	1.22-1.37
[10]	3239	135000	7.41×10^{-7}	1.29-1.39
[20]	1560	8000	1.25×10^{-5}	1.36-1.41
[21]	-	5200	1.92×10^{-5}	1.33-1.37
Proposed	475	3000	5.83×10^{-6}	1.31-1.35

IV. OPTIMIZATION

Increasing the silver layer thickness reduces loss depth for a fixed analyte RI, as illustrated in the Fig. 5. The reason for this is that as the silver layer thickness increases, the damping loss increases [3,4]. In addition, when silver thickness increases, the peak confinement loss shifts to a longer wavelength.

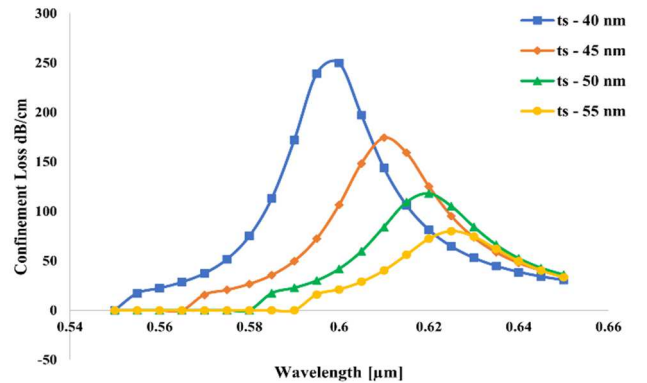


Fig. 5. Loss variation for different silver layer thicknesses for RI-1.33

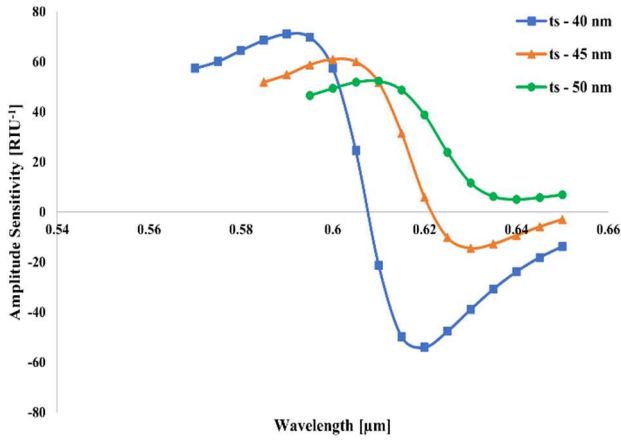


Fig. 6. Amplitude sensitivity for different silver layer thicknesses for RI-1.33

The sensor exhibits different S_A for silver layer thickness of 40, 45 and 50 nm. Maximum sensitivity was found at $t_s=40$ nm. That's why, throughout the performance analysis, $t_s=40$ nm was used.

The Confinement Loss for different TiO_2 layer thickness are shown in Fig. 7. The figure exhibits that for a fixed analyte RI, increasing the TiO_2 layer thickness increases confinement loss depth.

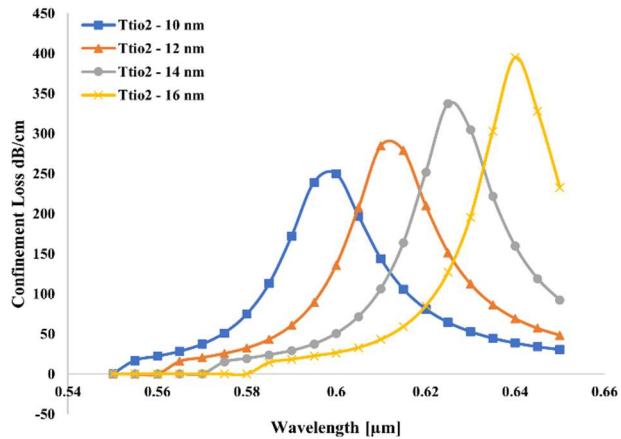


Fig. 7. Loss variation for different TiO_2 layer thicknesses for RI-1.33

But the proposed sensor shows quite similar amplitude sensitivity for TiO_2 layer thickness of 10, 12 and 14 nm, Fig. 8. Maximum sensitivity was found at $T_{TiO_2}=14$ nm of $175 RIU^{-1}$, while for $T_{TiO_2}=10$ nm is $162 RIU^{-1}$.

So, sensitivity quite close in range in both parameters. also keeping the TiO_2 layer thinner makes the sensor more effective in sensor resolution and SPP-mode generates more effectively. That's why, throughout the performance analysis, $T_{TiO_2}=10$ nm was used.

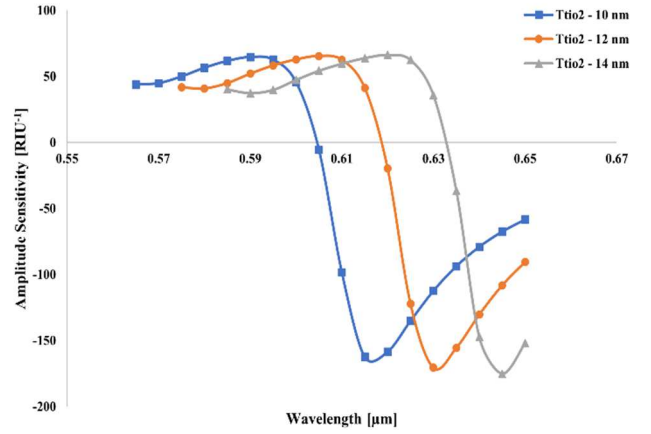


Fig. 8. Amplitude sensitivity for different TiO_2 layer thicknesses for RI-1.33

V. CONCLUSION

The proposed dual side polished PCF based Surface Plasmonic RI sensor was designed to detect water pollution at 1.33 RI unit. Using the wavelength interrogation method, the proposed sensor showed a maximum wavelength sensitivity of $3000 nm/RIU$ at a silver layer thickness of 40 nm in the sensing range of 1.31 to 1.35 RIU. At the target point 1.33 RIU for detecting water pollution, sensitivity of $2250 nm/RIU$ was observed. Hence, any change in the analyte (water) refractive index will be detected by this sensor. Furthermore, a maximum sensitivity of $475 RIU^{-1}$ and a maximum sensor resolution of $5.83 \times 10^{-6} RIU$ were obtained using an amplitude interrogation method. As the sensor showed promising data in other RI ranging from 1.31 to 1.35 RIU, this sensor can be used on those analyte range for other purposes.

REFERENCES

- [1] Emranul Haque, Subaha Mahmuda, Md. Anwar Hossain, Nguyen Hoang Hai, Yoshinori Namihira, Feroz Ahmed, "Highly Sensitive Dual-Core PCF Based Plasmonic Refractive Index Sensor for Low Refractive Index Detection". IEEE Photon. J., Vol. 11, No. 5, PP Oct. 2019.
- [2] B. Lee, S. Roh, and J. Park, "Current status of micro- and nano-structured optical fiber sensors", Optical Fiber Technology, vol. 15, no. 3, pp. 209–221, 2009 /intro, hgis.
- [3] Md. Rabiul Hasan, Sanjida Akter, Ahmmed A. Rifat, Sohel Rana and Sharafat Ali, "A highly sensitive gold-coated photonic crystal fiber biosensor based on surface plasmon resonance", Photonics 2017, 4, 18.
- [4] Abdullah Al Noman, Emranul Haque, Md. Anwar Hossain, Nguyen Hoang Hai, Yoshinori Namihira and Feroz Ahmed, "Sensitivity Enhancement of Modified D-Shaped Microchannel PCF Based Surface Plasmon Resonance", Optical Sensors 2020, 20(21), 6049.
- [5] Emranul Haque, Md. Anwar Hossain, Yoshinori Namihira and Feroz Ahmed, "Microchannel-based plasmonic refractive index sensor for low refractive index detection", Vol. 58, No. 6 / 20 February 2019 / Applied Optics.
- [6] Haque, E.; Hossain, M.A.; Ahmed, F.; Namihira, Y., "Surface Plasmon Resonance Sensor Based on Modified D-Shaped Photonic Crystal Fiber for Wider Range of Refractive Index Detection". IEEE Sens. J. 2018, 18, 8287–8293.
- [7] Wang, G.; Lu, Y.; Duan, L.; Yao, J., "A Refractive Index Sensor Based on PCF With Ultra-Wide Detection Range". IEEE J. Sel. Top. Quantum Electron. 2020, 27, 5600108.
- [8] Ruhul Amin, Lway Faisal Abdulrazak, Noor Mohammadd et al., "GaAs-filled elliptical core-based hexagonal PCF with excellent

optical properties for nonlinear optical applications", *Ceramics International*-Volume 48, Issue 4, 15 February 2022, Pages 5617-5625, doi.org/10.1016/j.ceramint.2021.11.106

- [9] J. Homola, "Surface plasmon resonance sensors for detection of chemical and biological species," *Chemical reviews*, vol. 108, pp. 462-493, 2008.
- [10] M. A. Hossain and Y. Namihira, "Center wavelength adoption techniques for supercontinuum generating highly nonlinear noncircular core photonic crystal fiber," *Jpn. J. Appl. Phys.* 52, 052502 (2013).
- [11] N. Mohammada, L.F. Abdulrazakb, S.R. Tahhan, R. Amin et al., "GaP-filled PCF with ultra-high birefringence and nonlinearity for distinctive optical applications", *Journal of Ovonic Research*, Vol. 18, No. 2, March - April 2022, p. 129 – 140
- [12] M. A. Hossain, Y. Namihira, S. M. A. Razzak, M. A. Islam, J. Liu, S. F. Kaijage, and Y. Hirako, "Design of all normal dispersion highly nonlinear photonic crystal fibers for supercontinuum light sources: applications to optical coherence tomography systems," *Opt. Laser Technol.* 44, 976–980 (2012).
- [13] Mohammad Al Mahfuz, Md. Anwar Hossain, Emranul Haque, Nguyen Hoang Hai, Yoshinori Namihira and Feroz Ahmed, "A bimetallic-coated, low propagation loss, photonic crystal fiber based plasmonic refractive index sensor", *Sensors* 2019, 19, 3794.
- [14] G. An, S. Li, H. Wang, X. Zhang, and X. Yan, "Quasi-D-shaped optical fiber plasmonic refractive index sensor," *J. Opt.* 20, 035403 (2018).
- [15] Homola, J., Ed., 2006. *Surface Plasmon Resonance Based Sensors* (Heidelberg, Germany, Springer). DOI: 10.1007/b100321. 4, 5.
- [16] Pitarke, J. M., Silkin, V. M., Chulkov, E. V., and Echenique, P. M. 2007. Theory of surface plasmons and surface-plasmon polaritons, *Rep. Prog. Phys.*, 70:1–87. DOI: 10.1088/0034-4885/70/1/r01.4.
- [17] Ruhul Amin, Lway Faisal Abdulrazak Enam Khana et al., "Inspection of an HSH-PCF for optical Communication with high non-linearity, birefringence and negative dispersion", *Alexandria Engineering Journal* (2022) 61, 11139–11147
- [18] Md. Aslam Mollah, S.M. Abdur Razzak, Alok Kumar Paul, Md. Rabiul Hasan, "Microstructure optical fiber based plasmonic refractive index sensor", *Sensing and Bio-Sensing Research* 24 (2019) 100286.
- [19] Tianshu Li, Lianqing Zhu, Xianchao Yang, Xiaoping Lou and Liandong Yu, "A Refractive Index Sensor Based on H-Shaped Photonic Crystal Fibers Coated with Ag-Graphene Layers", *Sensors* 2020, 20, 741.
- [20] M. R. Hasan, S. Akter, K. Ahmed, and D. Abbott, "Plasmonic refractive index sensor employing niobium nanofilm on photonic crystal fiber," *IEEE Photon. Technol. Lett.*, vol. 30, no. 4, pp. 315–318, Feb. 2018.
- [21] J. N. Dash and R. Jha, "Highly sensitive D shaped PCF sensor based on SPR for near IR," *Opt. Quantum Electron.*, vol. 48, no. 137, pp. 1–7, 20